SSRG International Journal of Electrical and Electronics Engineering
ISSN: 2348-8379/ https://doi.org/10.14445/23488379/IJEEE-V12I8P110

Volume 12 Issue 8, 99-111, August 2025

Original Article

Voltage Control and Reactive Power Support Optimization Using (SA-STO) Algorithm in Virtual Power Plants (VPPs)

Srinivasa Rao.Sureddy[1], Nageswara Rao.Pulivarthi[2]

[1,2]*Department of EECE, GITAM Deemed To Be University, Andhra Pradesh, India.*

[1]*Corresponding Author : ssureddy2@gitam.in*

Received: 07 June 2025 Revised: 09 July 2025 Accepted: 08 August 2025 Published: 30 August 2025

Abstract - *The complexity of voltage control and reactive power support has risen due to the increasing integration of renewable energy sources in Virtual Power Plants (VPPs). Therefore, effective management is vital for grid stability and energy optimization. To improve voltage control and reactive power management in VPPs, this research introduces a new method that uses the SA-STO algorithm. The proposed Self-Adaptive Siberian Tiger Optimization (SA-STO) algorithm continuously modifies its search parameters according to the power grid's operating circumstances to achieve adaptive and efficient optimization. The approach increases the stability of voltage profiles, speeds up convergence, and prevents local optima by using the self-adaptive mechanism. Many constraints are considered to optimize for both efficient energy use and grid dependability, such as reactive power compensation, voltage deviation reduction, and power flow balancing. Key results include a reduction in average voltage deviation by ~35%, a decrease in power loss from 12 kW to 1–2 kW, and convergence within ~100 iterations—outperforming PI, PID, and static FOPID controllers. Compared to traditional optimization approaches, the SA-STO algorithm achieves better simulation results for voltage regulation accuracy, computational resilience, and reactive power support efficiency. The results show that it might be an effective optimization tool for making current VPPs more efficient, leading to a more stable and renewable energy grid.*

Keywords - *Voltage control, VPPs, Reactive power, Optimization, Renewable energy.*

1. Introduction

Virtual Power Plants (VPPs) are in increasing demand in today's complex and decentralized power industry because of their ability to combine renewable energy resources and stabilize the grid. VPPs also play a significant role in bringing together Distributed Energy Resources (DERs), like producing Renewable Energy Sources (RES), storing energy, and shifting electricity usage depending on the grid's condition. The control of Voltage and Reactive Power (VRP) is responsible for characteristics in the supply of electricity, such as its quality of supply, dependence on resources, and stability (Goia et al.,2012). VPPs aid in enhancing the resilient nature of grids, making them more flexible and, at the same time, aid in balancing the demand for resources and the supply of the same. Virtual Power Plants (VPPs) combine different types of distributed energy resources, such as solar PV, wind turbines, energy storage (BESS), electric vehicles, and flexible loads, into one controllable unit that can take part in energy markets and offer extra services like voltage and reactive power control. This grouping allows power and information to flow in both directions, which makes VPPs more flexible but also harder to manage than traditional generation systems. Some of the main problems with controlling reactive power and voltage in VPPs are: A mixed-integer optimization problem, since VPPs coordinate discrete devices (like OLTC and capacitor banks) with continuous resources (like inverters). High penetration of inverter-based DERs causes reverse power flows and voltage instability, which traditional controllers like STATCOM or SVC have a hard time fixing on the fly. The reactive power capability of an inverter can change a lot based on the real power output and available capacity. This means that adaptive coordination is needed instead of static scheduling. These problems show how limited traditional Volt-VAR methods are and make it clear that we need real-time, self-adaptive optimization methods. For example, the proposed SA-STO algorithm adjusts search behavior on the fly to control reactive power and voltage in VPP environments with a lot of DERs. Reactive Power Support and Voltage Control (RPS & VC) management in the power supply, importantly in VPPs, is significant for maintaining the flow of voltage in the entire grid and decreasing the effects of fluctuations in the output of RES (Enokido et al., 2011). Strong VM can help decrease the losses occurring in the system and enhance the transmission of power

and its efficiency in distribution; RP is crucial for regulating voltage (Stanelyte Radziukynas2020). VRP is an important and essential process for managing the inclusion of RES like wind and solar power for better efficiency of its operation and for being stabilized in nature (Ristono& Budi, 2025). The aspects mentioned above directly impact how the operations in the grid perform, how efficient they are, and their dependence on other resources; therefore, it is of utmost importance to perform optimization with a framework like VPPs (Callaway &Hiskens, 2011). Stabilized voltage graphs and a balance of RP will require an advanced VPP operation as the RES becomes more generalized.

The VPPs are constantly shifting and becoming more complex. Hence, the traditional optimization solutions for RPS and VC are less efficient. Yet another reason for their inefficiency is the characteristics of the grid-like, showcasing a behavior that is not linear and having a production of Renewable Energy (RE) that is unpredictable (Suresh & Lenine, (2024)). Because of the above-mentioned reasons, it is essential to have advanced optimization techniques that cater to real-world needs (Kadhim et al., 2024).

One advanced technique proposed for RPS & VC is the Self-Adaptive Siberian Tiger Optimization (SA-STO) algorithm. Compared to the optimization techniques used traditionally, this algorithm shows adaptivity towards varying situations of systems and more substantial outcomes and quickens convergence (Niknam et al., 2013). In accordance with the increased quality of the decisions made in systems like power grids with high complexity, this approach is an idea obtained from Siberian tigers that used an adaptive method of hunting. Because of its adaptive quality, the SA-STO is dynamic and can alter how it performs according to the changes in the condition of the system, making it suitable for the unpredictable and constantly changing market of RE. Researchers have recently used meta-heuristic algorithms like PSO, GA, and hybrid FOPID-based controllers to improve voltage and reactive power control in VPPs. However, many studies have not looked at how these algorithms can change on the fly to deal with the quickly changing operating conditions that are common in VPP environments, like changing load, renewable energy injection, and grid problems. Because of this, traditional methods often take a long time to converge and run the risk of getting stuck in local optima. To improve both the speed of convergence and the quality of the solutions for reactive power dispatch and voltage control in VPPs, this study suggests the Self-Adaptive Siberian Tiger Optimization (SA-STO) algorithm. This algorithm changes its search parameters in real time based on grid conditions.

2. Literature Review

Many recent studies have explored different ways to control voltage in power and electric systems, more importantly, during the integration of RE. VC is significant for maintaining the stabilization of systems and enhancing how they perform. A study by Fusco et al. (2021) described a mechanism as a decentralized approach for VC in newer grids with RESs. This mechanism uses classical control strategies, like transformer tap changers, and advanced methods, such as Battery Energy Storage Systems (BESS), which help stabilize the real-time voltage. Managing voltage in VPPs is more difficult because they integrate DERs like wind energy, solar energy, and systems for storage (Rajput et al., 2024). The details on how VC can be optimized using VPPs using a versatile approach called Dynamic Voltage Regulation (DVR) using information like the grid condition, generation profile, and load were researched (Huang & Zhang, 2025). This approach works by adjusting the regulating actions of the DERs through a communication system.

RP stabilizes voltage and ensures that the power flow in grids is efficient. Traditional techniques used in the RP compensation process, like the (Static VAR Compensators STATCOM) and Static VAR Compensators (SVC), are still available. However, they are not very adaptive and require change according to the condition of the systems. Recent research by Dawn et al. (2024) talked about the need for compensation systems for RP with high adaptability and intelligence, especially during the integration of RES, which has power outputs.

In cases where RES like wind and solar are integrated, the RPS in VPPs ensures grid stability and reliability. In 2024, (Sikorski et al. 2020) researched how DERs in VPPs can independently lend a hand to RPS by controlling the local inverters. This study found that a decentralized approach to RP management can improve the grid's performance at minimal costs of operation and minimal losses.

With an increase in decentralized VPPs, the deniability of VPPs has become more popular. In 2023, Researchers Wang et al. established a framework for optimization that is hybrid, meaning that it combines operational and market-based approaches. This approach facilitates the integration of RP control and enhances the system's efficiency. This framework utilizes optimized algorithms, instantaneous forecasting, and price signals to efficiently dispatch energy resources and maintain RPS and VC. One major challenge in VPPs while managing RP and controlling voltage is coordinating different resources. A study by Marinescu et al. (2022) focused on developing an approach for VPPs that performs optimization on both the dispatch of energy and the compensation of RP simultaneously. To reduce the loss of power and increase the stability of the system, this approach used an algorithm for optimization.

The SA-STO algorithm implements a technique for optimization, which was inspired by the Siberian Tigers Hunt. This algorithm works in a way that adjusts its parameters for searching based on the context of the problem, thus enhancing the rate of convergence and providing a better trade-off

between exploitation and exploration. In a study in 2023 by Iqbal et al. (2024), a hybrid algorithm was introduced, which involves different techniques like GA techniques d PSO with the SA-STO for enhanced performance. This form of an algorithm provides optimal solutions, more efficient convergence, and less computational time. However, another evolving area of research is the integration of technologies that use smart grids with VPPs. A study in 2024 by Michael et al. (2022) showed that the interaction of smart grids with VPP provides a platform for active adjustments in RPS and voltage. This study ensures proper energy distribution, efficient optimization, and stabilization of voltage levels.

Table 1. Related works of the proposed model

S.no	Authors (Year)	Methodology	Key Contributions	Identified Gaps
1	T. Vafa, M. H. Ershadi & B. Arandian (2025)	AC-OPF reactive and active dispatch in VPP considering smart inverter services	Integrated reactive power dispatch with ancillary services; <0.015 pu voltage regulation in IEEE test systems	Focused on deterministic OPF; lacks online/adaptive metaheuristic tuning capability
2	B. Goia, T. Cioară& I. Anghel (2022)	Narrative review of VPP optimization techniques and services	Categorized VPP methods across markets, control, and DER coordination	Descriptive, not quantitative; lacks detailed discussion on algorithmic adaptability
3	Mohammed et el (2024) (Energy Informatics)	Literature review of reactive power planning strategies in microgrids	Synthesized 20 recent studies; highlighted voltage stability improvements from strategic RPP	Focus is on planning, less on real-time control or algorithm comparison
4	M. Almomani, A. Alkhonain& V. Ajjarapu (2025)	Sensitivity-aware reactive dispatch using smart inverters in VPPs	Achieved dynamic VPP voltage control via smart inverter modes; performance validated on IEEE-13 and 123 systems	Emphasizes sensitivity-based dispatch; not employing autonomous metaheuristic adaptation
5	Esfahani et al. (2023)	Dynamic Volt-VAR scheduling in microgrids using chance-constrained optimization	Proposed robust prosumer co-optimization under uncertainty; scalable VPP scheduling	No reactive power control algorithm comparison; static scheduling rather than adaptive control

Table 1 demonstrates the related works done by various authors. Vafa et al. (2025) show how smart inverter coordination in VPPs can effectively regulate voltage, but their approach is predicated on deterministic AC-OPF optimization. While reviewing various VPP optimization techniques, Goia et al. (2022) point out the need for more flexible algorithmic solutions. Reactive-power planning techniques without online control mechanisms are highlighted by Mohammed et el (2024). Despite not having runtime parameter self-tuning, Almomani et al. (2025) offer a sophisticated sensitivity-based dispatch for smart inverters. Using prosumer co-optimization without adaptive reactive-power controllers, Esfahani et al. (2023)tackle scheduling under uncertainty. These studies collectively highlight the need that SA-STO addresses by providing real-time adaptive optimization for reactive-power and voltage control in dynamic VPP environments.

To reduce voltage deviations and reactive power losses, the majority of previous studies on Volt-VAR control in VPPs employ metaheuristic algorithms such as PSO, GA, and ABC (Stanelyte&Radziukynas, 2020; Bakare et al., 2007; Mourtzis et al., 2023; Nezamabadi et al., 2016). However, under variable renewable conditions, these approaches often rely on fixed tuning parameters, which limit their adaptability and may result in slow convergence or becoming trapped in local optima (Eghbal et al., 2008). While recent Deep Reinforcement Learning (DRL) techniques like DQN, DDPG, SAC, and MACSAC provide greater real-time flexibility, they must be trained on large datasets and are primarily tested on static feeders rather than fully dynamic VPPs (Zhang et al., 2020; Gao et al., 2020; Esfahani et al., 2023). But the proposed Self-Adaptive Siberian Tiger Optimization (SA-STO) does not require offline training or manual parameter tuning, instead, it modifies its search parameters online in response to real-time grid feedback. In dynamic, renewable-rich VPP environments, this self-adaptive mechanism provides faster convergence, improved escape from local optima, and increased robustness, providing definite advantages over both static metaheuristics and data-intensive DRL techniques.

2.1. Proposed Model

This study uses a new algorithm called the Self-Adaptive Siberian Tiger Optimization (SA-STO) to optimize voltage management and reactive power support in VPPs, illustrated in Figure 1. Energy storage devices, variable loads, and renewable power sources like solar and wind are all parts of the Distributed Energy Resources (DERs) that VPPs combine. Stable voltage levels, minimal reactive power losses, and maximum usage of renewable energy sources are all goals of these systems, which need effective optimization methodologies. The proposed method uses the SA-STO algorithm's adaptive features based on how Siberian tigers hunt. The optimization process is managed by this algorithm in a balanced way, with an exhaustive search for optimum solutions and a refinement of the search around desirable areas

in the solution space. By analyzing the VPP's real-time data, the algorithm makes adjustments to the reactive power output and voltage setpoints in real-time to keep the system stable. The approach offers a solid foundation for enhancing the stability and efficiency of energy distribution in VPPs by integrating power flow analysis with sophisticated optimization methods. Several case studies show that the method works well with variable renewable energy output, load demand, and operating circumstances, validating its efficacy in improving system performance.

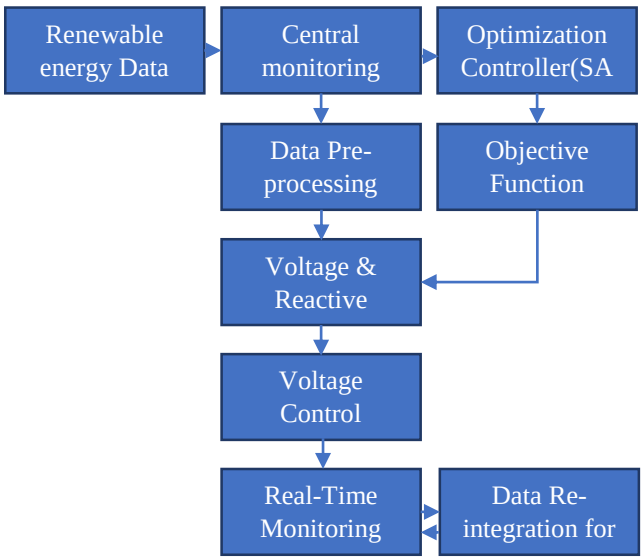

Fig. 1 Implementation flow of the proposed model

3. Model Description

A customized IEEE-33-bus distribution test system, as referenced in Stanelyte & Radziukynas (2020), is used to model the VPP environment. To simulate a real-world DER deployment, the VPP incorporates five DER units throughout the network: two 500 kW solar PV arrays, one 1 MW wind turbine, and two 200 kWh battery storage systems connected at strategic buses. Synthetic Weibull-distributed wind-speed models and half-hourly solar irradiation data were used to create profiles of renewable generation. Based on regional utility data, load demand profiles show the total amount of residential, commercial, and industrial usage over a 24-hour period. Every simulation was carried out using MATLAB Simulink (R2022a) with EVAT network modelling on a Windows 10 Pro computer (Intel Core i3 @ 3.60 GHz, 8 GB RAM). To support reproducibility, the supplementary materials include input-profile files, DER specifications, and detailed system parameters.

3.1. Hybrid PI-FOPID Controller

The main aim of having this controller design that has been proposed is to check the response of the frequency of the hybrid microgrid in situations where disruptions in load take place and when there are variations in Renewable Energy Sources (RES). This controller is proposed to decrease the power variations in the tie-line and reduce the frequency deviations. A control in the frequency is acquired because of the hybrid controller, which has both a PI controller and an FOPID controller. When a high percentage of resources have renewables, a decrease in power fluctuation in the tie-line and a deviation in frequency will prove to be significant. In this controller, the output obtained from the PI is taken as a set point by the FOPID controller. The hybrid controller is more productive than the single-loop controller because the system's performance is more efficient as it aids in decreasing the disturbances on secondary variables, which can affect the primary output process. It also decreases the impact of variations on the performance of the system. In the proposed control system's architecture, two controllers are present, and the output of one of the controllers handles the set point of another controller. The controller that regulates a set point is called the outside controller, or the significant or master controller. The controller where the set point is received is called the secondary controller, also called the inner or slave controller. Figure 2 shows the structure of the hybrid PI-FOPID controller.

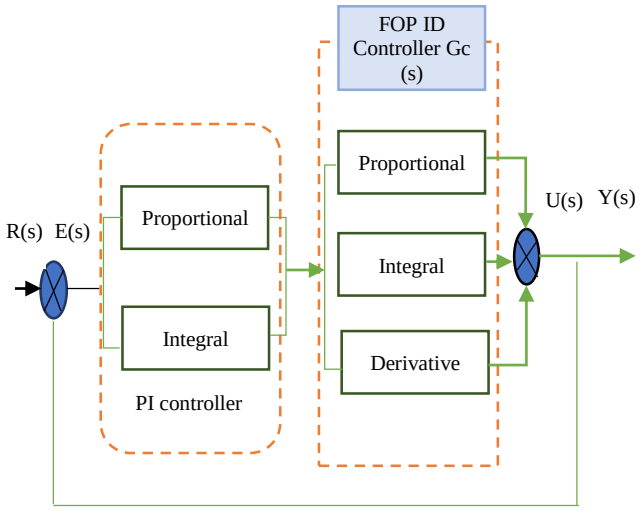

Fig. 2 Architecture of hybrid PI-FOPID

3.1.1. PI Controller

The signal indication R(s) refers to the input. The control system would either have this power output as the target it wants to reach, or this could be the optimal frequency it would want for a VPP system. The system will attempt to see if the input reference matches the actual output denoted as Y(s) because the RESs are often subjected to changes. The equation E(s) = R(s)-Y(s) is used to denote the difference in the actual output of the system from the input reference. The controller functions in such a way that it reduces errors and gets an output from the system that is close to the value that is supposed to be gained. The initial part of the control block has PI. It exercises E(s), an error signal, to generate a control signal immediately. The reason why PI is popular is that it is easy to use and also because of its ability to handle steady-state errors. The (K_p), which is a proportional term, helps

enhance the overshoots and response of the rise time, whereas the (K_i), which is an integral term that helps greatly reduce steady-state errors. A high proportional gain value is required to have a good control effect, especially when the speed error is huge. Also, a significant value of integral gain is required to reduce steady-state errors when the speed error is less. Equations (1) and (2) depict the PI's output, the torque component used as a reference by the motor, and the transfer equation, respectively.

$$C_{PI(t)} = K_p(t)e(t) + K_I(t) \quad (1)$$

$$U_{PI}(S) = K_{p1}E(s) - \frac{K_I 1}{s}E(s) \quad (2)$$

Here, the proportional gain is denoted as $K_p(t)$, the integral gain is denoted as $K_i(t)$, and also $e(t) = w_r^*(t) - w_r(t)$. Improvements depend on e(t), which is the speed error. In Equation (3), the $K_p(t)$ is denoted as the speed error function.

$$K_p(t) = K_{p(max)} - \left(K_{p(max)} - K_{p(min)}\right)e^{-[ke(t)]} \quad (3)$$

The k is used as a constant to determine the rate of difference of $K_p(t)$ between the proportional gain's minimum value and maximum value. To get a fast transient response while having a high et(t), which is speed error,$K_{p(max)}$, which is a proportional gain of high value, is employed, and whenever e(t) is considerably less, to eliminate overshoots and also oscillations, the $K_{p(min)}$, which is a proportional gain of low value, is used. Equation (4) shows the relation between e(t) and integral gain, which is denoted as

$$K_i(t) = K_{i(\max)}e^{-[ke(t)]} \quad (4)$$

An integral gain of high value is included when e(t) in steady-state conditions is considerably small to compensate for errors that are in steady-state. Whenever the error is large, an integral gain of a small value is brought into action to eliminate oscillations that are not required and unwanted overshoots. A huge control signal is utilized in transient conditions to accelerate or decelerate a motor within a short duration to a pre-referenced value. During this process, $K_p(t)$ tends to reach a higher value, and $K_i(t)$ tends to remain at a low value. $K_i(t)$ reaches its maximum level during steady-state operation.

3.1.2. FOPID Controller

Fractional Order PID, also known as the FOPID controller, is more advanced than the traditionally used PID controller, constituting the second block of controllers. The flexibility and regulation of complex functions of the system are carried out by including a fractional calculus in the processing part of this controller. A non-integer order is utilized for proportional components, derivatives, and integrals used in FOPID, making it a more expanded and complex version of the traditionally used PI. The ability of this controller to govern complex systems and modify systems that include factors like dynamics that have an ordering of non-integers, are non-linear and have time delays increases its degrees of freedom. The non-local dynamics are seen in FOPID compared to its counterparts with integer order, indicating that it is also important to analyze the history of error signals when determining the proper action to be taken. FOPID has become more popular because of its resilient nature and enhanced performance. Equations (5) and (6) show how the calculation of a controller gain, along with the transient equation, is performed.

$$C_{FOPID}(t) = K_P + K_I\frac{1}{s^{\lambda}} + K_D s^{\mu} \quad (5)$$

$$U_{FOPID}(S) = K_{P2}E(s) + K_I\frac{1}{s^{\lambda}}E(s) + K_{D2}s^{\mu} \quad (6)$$

Here, the output of the controller is denoted as Y(s), the input of the controller as U(s), and the controller's transfer function is G_c. K_I is used to represent fractional parts of integral controllers, and K_D is used to represent derivative controllers along with their gains. They are denoted as λas well as μ, respectively. K_P is also known as proportional gain. U(s) is used to indicate the error between actual values and desired values. The role of PI is to reduce the increased errors that occur initially, after which FOPID uses advanced dynamics, which are of the fractional-order type, to refine the output. Compared to PI, the FOPID is more robust because of the availability of fractional parts in the controller. High versatility is achieved with the use of controllers that have terms of fractional order, like s^{μ} as well as sλ in comparison with controllers that have integer order. Therefore, dynamic and complex systems with RESs like the VPPs use FOPID. Specifically, FOPID can take care of non-linearities as well as uncertainties during the process of producing renewable energy. In Equation (7), U(s), the output from the hybrid controller, is the signal acquired from FOPID and PI. This output signal is fed into the VPP system to see how it behaves and generate an actual outcome called Y(s), the reference input in the close margin with R(s).

$$U(s) = U_{PI}(S) + U_{FOPID}(s) \quad (7)$$

The optimization of parameters like μ, λ, K_{p1}, K_{p2}, K_{I1}, K_{I2}, and K_D will help in ensuring a performance that is optimal for the required tasks. An algorithm called the Self Adaptive Siberian Tiger Optimization (SA-STO) is implemented to obtain values that are ideal for the above parameters. The aim of bringing in SA-STO is to use it to decrease the loss occurring in VPP by tuning the FOPID parameters. To add to that, it also makes sure that the RESs are used efficiently, and at the same time, it makes sure there is proper stabilization in the system. This impacts electric power deviations in tie-lines, ultimately decreasing the loss of power. The reduction in loss of power is described as follows in Equation (8):

$$\min P_{loss} = f(K_P, K_I, K_D, \lambda, \mu) \quad (8)$$

Here the

$$K_P^{min} \le K_P \le K_P^{max}$$
$$K_I^{min} \le K_I \le K_I^{max}$$
$$K_D^{min} \le K_D \le K_D^{max}$$
$$0 \le \lambda \le 20 \le \mu \le 2$$

The SA-STO performs its task by adjusting parametersμ, λ, K_P, K_D, and K_I, increasing optimization and decreasing power loss. The PI and FOPID controller parameters, namely the gains K_P, K_I, K_D and the fractional orders λ and μ are optimally tuned using the SA-STO algorithm. The inner FOPID controller in the hybrid architecture uses fractional dynamics to refine the transient response, while the outer PI controller corrects steady-state errors. In order to minimize power loss and voltage deviation, SA-STO dynamically modifies these parameters in real time based on grid feedback. Under a variety of operating conditions, this structured control scheme guarantees robustness and quick convergence.

3.2. Self-Adaptive Siberian Tiger Optimization (SA-STO)

The algorithm SA-STO is a metaheuristic approach to optimzing parameters involved in hybrid PI-FOPID. The idea for this approach was adapted from survival techniques and natural hunting methods implemented by Siberian tigers, and it uses the phases called bear combat and prey hunting. The tigers determine the best possible solutions when optimization takes place, allowing them to decide on a position and adjust to it with respect to the values of the objective function. The process of determining positions and adjusting to them has two stages, and these are based on the animal's natural hunting activity.

3.2.1. Initialization

The STO's repetitive process, which utilizes the population's search ability, can provide an effective and feasible solution to the problem. The Siberian tigers, which are a part of the population of STO, have the habit of roaming around a search space to obtain efficient solutions. All Siberian tigers are a part of the population, so they can provide a potential solution. By assigning matrices to the population and vectors to every individual, a mathematical model exclusively for Siberian tigers can be formed, as depicted in Equation (9). The values assigned to the variables of the problem are indicated by the location within the area it searches.

$$ST = \begin{bmatrix} ST_1 \\ \vdots \\ ST_i \\ \vdots \\ ST_N \end{bmatrix}_{N\times m} = \begin{bmatrix} st_{1,1} & \cdots & st_{1,j} & \cdots & st_{1,m} \\ \vdots & \ddots & \vdots & \iddots & \vdots \\ st_{i,1} & \cdots & st_{i,j} & \cdots & st_{i,m} \\ \vdots & \iddots & \vdots & \ddots & \vdots \\ st_{N,1} & \cdots & st_{N,j} & \cdots & st_{1,1} \end{bmatrix}_{N\times m} \quad (9)$$

The population matrix of the locations of Siberian tigers is denoted as ST, the i^{th} tiger is denoted as ST_i, which will provide a feasible solution, and the total number of tigers is denoted as N. The random spots where the Siberian tigers are placed initially in the search area after the application of STO are determined by Equation (10).

$$ST_{i,j} = LB_j + r_{i,j}.\left(UB_j - LB_j\right), \quad i = 1,2,\ldots,N; j = 1,2,\ldots\ldots,m \quad (10)$$

Here, the values that are arbitrary within the interval of [0;1] are denoted as $r_{i,j}$, the LB_j andUB_j are the lower bound and upper bound of the j^{th} problem variable,$ST_{i,j}$ denotes ST_i's j^{th} dimension in the search area, which is the problem variable, and the count of issue variables is denoted as m. The location of the Siberian tiger in the search area is determined with the help of the problem variable's values. Hence, for all Siberian tigers, a particular value for the objective function of the problem can be determined. For the objective function, a group of values that are determined can be denoted with the help of a vector, also known as an objective function vector, which is depicted in Equation (11).

$$F = \begin{bmatrix} F_1 \\ \vdots \\ F_i \\ \vdots \\ F_N \end{bmatrix}_{N\times 1} = \begin{bmatrix} F(ST_1) \\ \vdots \\ F(ST_i) \\ \vdots \\ F(ST_N) \end{bmatrix}_{N\times 1} \quad (11)$$

Here, the obtained value of the objective function for the i^{th} tiger is F_i, and F is the vector of the values of the objective function.

3.2.2. First Phase: Chaotic Prey Hunting

Siberian tigers are pretty strong predators as they can attack diverse prey species. So, the members of STO get updates by copying the hunting techniques used by Siberian tigers. The steps involved in this technique include fixing a target, going for the attack, and going after it until it is taken down or killed. Hence, the phase of hunting a prey has two segments. Stage one involves updating the position of the population depending on the selection and attack planned on the prey.

This stage will have important and sudden shifts in the positions of the members of STO, which will tune the capacity of the algorithm, making it ready for global exploration, searching, and scanning the search space in a precise manner. All Siberian tigers in the STO model will suggest locations of prey chosen from the population's members who have an objective function larger than that of an individual. Equation (12) displays the suggested positions of the prey.

$$PPrey_i = \{ST_k | k \in \{1,2,\ldots,N\} \wedge F_k < F_i\} \cup \{ST_{best}\} \quad (12)$$

Here, the best candidate solution is denoted as ST_{best}, and the i^{th} a member of the population, which is i^{th} tiger, picks any one member in a random manner in the set denoted as $PPrey_i$ for the attack, the simulation of the attack, and the calculation of the current location of the prey.

$$ST_{i,j}^{P1S1} = ST_{i,j} + r_{i,j}.(TP_{i,j} - I_{i,j}.ST_{i,j}) * Z_{i+1} \quad (13)$$

$$Z_{i+1} = \cos(w * cos^{-1} z_i) \quad -1 \leq z_i \leq 1; w \in [2,6] \quad (14)$$

Here, the set has random numbers denoted as $I_{i,j}$, and Chebyshev chaotic map is denoted in Equation (14) as $\{1,2\}.Z_{i+1}$. This map is to introduce an attack simulation that is unpredictable and random. It enables the algorithm to search various parts of the area and does not let it linger in an optimum local to the members. Based on the first phase and stage of STO, the i^{th} member's location is denoted as ST_i^{P1S1}, and its j^{th} dimension is denoted as $ST_{i,j}^{P1S1}$ in Equation (14).

If there is an increase in the objective function's value when the new position is calculated, then it will be accepted during the procedure of updating STO members. This process is denoted in Equation (15).

$$ST_i = \begin{cases} ST_i^{P1S1}, & F_i^{P1S1} < F_i \\ ST_i, & else \end{cases} \quad (15)$$

Here, the i^{th} member is F_i^{P1S1}, and the value of the objective function is ST_i^{P1S1}. As indicated in the protocol, the position of members in the population is updated in the second phase. In this phase, the tiger alters its position in the space where the prey is being attacked. This procedure helps enhance the algorithm's ability to predict better solutions in local exploitation and search.

The new location of the tiger, which is close to the site where the attack took place, is determined by Equation (16), which is determined so that it can be used for the upcoming chase or attack. After that, if there is an increase in the objective function's value, then the previous position of the member is replaced by the location, which is computed anew, as depicted in Equation (17).

$$ST_i^{P1S2} = ST_{i,j} + \frac{r_{i,j}.(UB_j - LB_j)}{t} \; ; t=1,2\ldots., T \quad (16)$$

$$ST_i = \begin{cases} ST_i^{P1S2}, & F_i^{P1S2} < F_i \\ ST_i, & else \end{cases} \quad (17)$$

Here, between intervals [0;1], there are random integers denoted as $r_{i,j}$. The algorithm's iteration counter is denoted as t. The objective function's value is depicted as F_i^{P1S2}. The i^{th} tiger's new location is denoted as $ST_{i,j}^{P1S2}$, and the j^{th} dimension is ST_i^{P1S2} based on stage two in phase one. Figure 3 shows the SA-STO's flow chart.

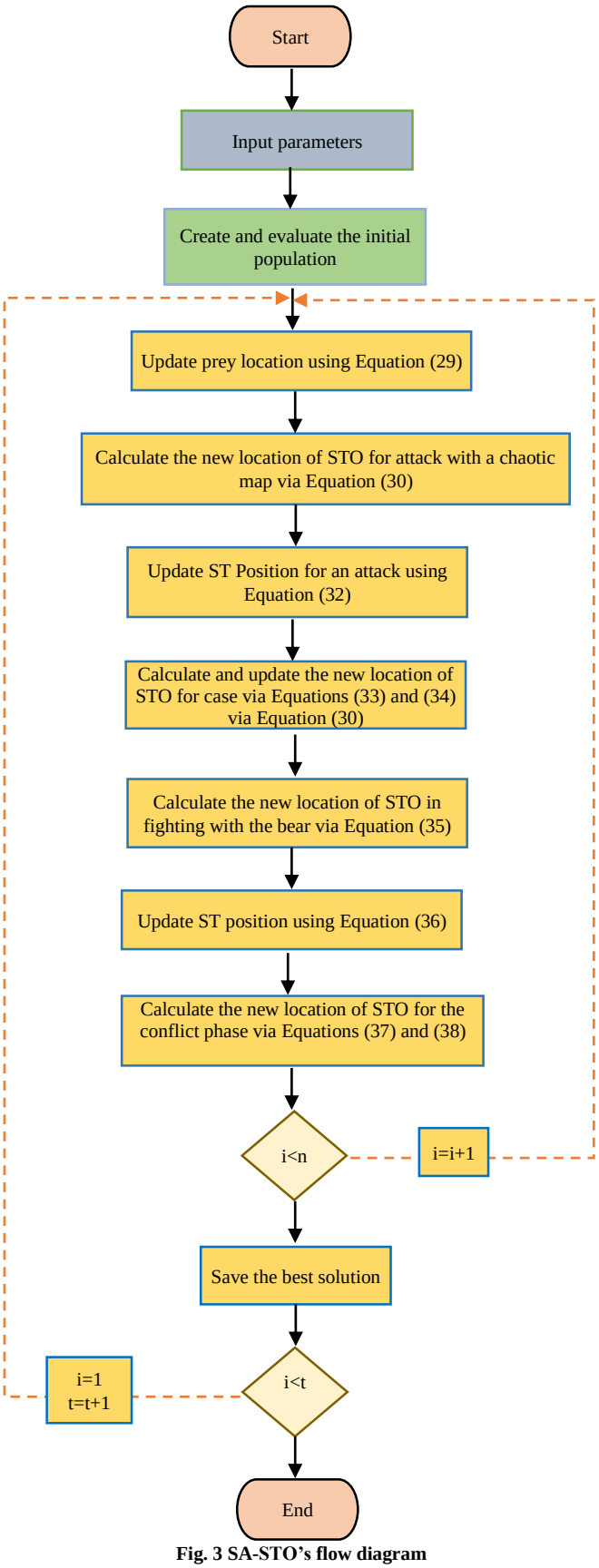

Fig. 3 SA-STO's flow diagram

3.2.3. Second Phase: Combat with a Bear

It is observed that, to resolve food conflicts and have their territory defended, Siberian tigers combat brown bears and black bears within their environment. In phase two, STO members are upgraded to develop the techniques used by the tigers during bear combat. The bear is ambushed in the fight before it gets struck by the tiger. This battle between the tiger and the bear does not cease until the tiger goes for the kill. Hence, the simulation of the attack in 2 phases and the simulation of the battle approach take place.

In stage one, the rest of the individuals in the community are considered as a bear set, and it creates a condition for an attack on a bear by i^{th} tiger. 'k' is used to denote the random position of the bear that has been assaulted, which is picked from a set of bears having the potential. This particular stage significantly impacts the STO members' positions, which change abruptly, enhancing the whole strategy by attaining global exploration ability. Therefore, Equation (18) is implemented to determine a new location for STO's i^{th} member to imitate previously used ideas.

$$ST_{i,j}^{P2S1} = \begin{cases} ST_{i,j} + r_{i,j}.\left(ST_{k,j} - I_{i,j}.ST_{i,j}\right), F_k < F_i \\ ST_{i,j} + r_{i,j}.\left(ST_{i,j} - I_{i,j}.ST_{k,j}\right), else \end{cases} \quad (18)$$

Here, from the set {1,2, …., $i-1$, $i+1$, …, N}, k is randomly selected; bear site's j^{th} dimension is denoted as $ST_{k,j}$, concerning phase two in stage one, the new location of i^{th} member is depicted as *j = 1, 2..., m.*$ST_{i,j}^{P2S1}$. j^{th} dimension is $ST_{i,j}^{P2S1}$. $r_{i,j}$ are random numbers between [0;1]. Set {1,2} has random numbers represented as $I_{i,j}$. Equation (19) interprets the information of the replacement of the location used previously by a member with a position that is freshly computed when the value of the objective function is increased.

$$ST_i = \begin{cases} ST_i^{P2S1}, & F_i^{P2S1} < F_i \\ ST_i, & else \end{cases} \quad (19)$$

Here, ST_i^{P2S1}'the objective function value is denoted as F_i^{P2S1}, and the bear's objective function value is denoted as F_k, which is STO's k^{th} member. Through modeling the battles that take place, the location of the population is updated in step two. Because of this, the positions of the population members vary, making the STO's capability of exploration and local search stronger. To carry out this process, a random placement near the combat site is first figured out with the help of Equation (20).

$$ST_{i,j}^{P2S2} = ST_{i,j} + \frac{r_{i,j}.(UB_j - LB_j)}{t} \quad (20)$$

Where the iteration counter of the algorithm is denoted by t,$ST_{i,j}^{P2S2}$is the new location of the tiger and its j^{th} dimension based on phase two and stage two of STO. According to Equation (21), for the process of updating, the value of the objective function must be increased because of the new position.

$$ST_i = \begin{cases} ST_i^{P2S2}, & F_i^{P2S2} < F_i \\ ST_i, & else \end{cases} \quad (21)$$

Here, F_i^{P2S2} is the value of an objective function of ST_i^{P2S2}.

Algorithm 1: Proposed Algorithm

Parameters have to be initialized:

1. The size of the population has to be initialized by the variable N
2. The maximum count of iterations has to be set as $\max_{iter}$
3. Exploitation rate (β) and exploration rate (α) must be defined.
4. Reactive Power's solution bound should be set as $Q_{min}$and Q_{max}, and for Voltage, it should be set as $V_{min}$and V_{max}.
5. The population of potential solutions has to be initialized as X (values of Reactive Power (RP) and Voltage(V)).

Evaluate the Initial population's fitness

6. A function for fitness has to be defined, i.e. F(solution):

- F(solution) = $\Sigma\ (V_i - V_{set})^{\ 2} + \Sigma\ (Q_j - Q_{set})^2$

In which:

- voltage at the i^{th} bus is denoted as V_i
- optimal setpoint for voltage is denoted as V_{set}
- reactive power at j^{th} bus is denoted as O_j
- optimal setpoint for reactive power is denoted as O_{set}

7. For every potential solution by individuals belonging to Population X:

a. Fitness function has to be used for evaluating the fitness F(Solution)

Main optimization loop:

8. For iteration from t=1 till $\max_{iter}$:

a. **Exploration Phase**:

- For every potential solution by individuals belonging to Population X:

i. The solution (RP and V) has to be adjusted randomly on the basis of the rate of exploration

ii. A re-evaluation of fitness F(solution) has to be done

iii. Newly obtained values have to be updated in the solution in case F(solution) is more accurate than the previous time

b. **Exploitation Phase**:

- For every potential solution by individuals belonging to Population X:

i. Exploitation rate β must be used for refining solutions by making adjustments in solutions that are the best

ii. A re-evaluation of fitness F(solution) has to be done

iii. Newly obtained values have to be updated in the solution in case F(solution) It is more accurate than the previous time.

c. **Selection**:

- For the formation of the next generation, values having the lowest fitness have to be selected from population X, as they are the solutions that are best

- Low optimal solutions have to be replaced by those that perform the best.

d. **Crossover**:

On the parent solution set, a recombination technique, also known as crossover, has to be applied to combine the parents' features to obtain solutions for offspring.

e. **Mutation**:

Mutation has to be applied by randomly altering offspring so that population diversity remains intact.

f. **Update Population**:

The population has to be updated periodically by replacing old solutions with new ones developed by mutation and crossover.

g. **Adaptive Parameters**:

- For the balance of local refinement and global search, the rate of exploitation β and the rate of exploration α have to be adjusted.

9. **Convergence Check**:

- If the value of best fitness does not improve in the previous iterations or if the iterations have reached their maximum point, the algorithm must be stopped.

10. **Return Optimal Solution**:

- The best solution amongst the many should be returned (VP setpoints and RP dispatch values) as optimized system settings.

End of Optimization.

3.3. Reactive Voltage Control Auxiliary Service Model for Virtual Power Plants (VPPs)

While dealing with issues regarding Reactive Voltage Control (RVC) in VPPs, the availability of devices that are adjustable in both discrete and continuous form suggests that RVC is a mixed-integer non-linear problem. Table 1 depicts the reactive devices that are adjustable and their features in a network of active distribution having many VPPs. The description of constraints and the objective function is given below. The proposed model is explained in Algorithm 1.

3.3.1. Objective Function

The system's reliability on an overall scale would be hard to ensure by simply using the active power optimization scheduling to pursue the hike in economic benefits. Hence, to optimize Reactive Power (RP) and maintain the quality of power, it is important to control and regulate the reactive devices that are adjustable in the distribution network inside VPPs. A significant indicator of the quality of power is the degree of deviation of voltage when measuring the quality of power. Therefore, the aim is to reduce the deviation in voltage on an overall scale in a network of active distribution with many VPPs, which develops the objective function depicted in Equation (22).

$$min \sum_{t=1}^{T} \left[\sum_{i \in N^D} \left(V_{i,t} - 1\right)^2 + \sum_{j=1}^{n} \sum_{g \in N_j^M} \left(V_{g,t} - 1\right)^2 \right] \quad (22)$$

In the above equation, the magnitude of voltage per unit at the nodes at time *t* is denoted as $V_{I,J}$, distribution network nodes as N^D, the number of VPPs as *n*, and the group of nodes for VPPs *j* is as N_j^M, the total number of control periods in a day is denoted as *T*.

3.3.2. Constraints

Constraints Power Flow

For the optimization of RP, certain constraints in power flow have to be followed, and they are depicted in Equation (23).

$$\begin{aligned} P_i^g + \sum_{m:m\to \mathrm{i}} P_{mi} &= \sum_{\mathrm{j:i}\to \mathrm{j}} P_{i,j} + P_i^{load} \\ Q_i^g + \sum_{m:m\to \mathrm{i}} Q_{mi} &= \sum_{\mathrm{j:i}\to \mathrm{j}} Q_{i,j} + Q_i^{load} \end{aligned} \quad (23)$$

$$\begin{aligned} P_{ij} &= V_i V_j \left(G_{ij} cos\theta_{ij} + B_{ij} sin\theta_{ij}\right) \\ Q_{ij} &= V_i V_j \left(G_{ij} sin\theta_{ij} - B_{ij} cos\theta_{ij}\right) \end{aligned}$$

In the equation above, the reactive power (RP)and active power (AP) are denoted as Q_i^g and P_i^g, and they are injected into bus *i.* At *I*, the reactive and active loads are denoted as Q_i^{load} and P_i^{load}. AP that passes in and out of *i*is denoted as $\sum_{m:m\to \mathrm{i}} Q_{mi}$ and $\sum_{m:m\to \mathrm{i}} P_{mi}$. The voltage in bus *i* and *j* is denoted as $V_i$and V_j. The RP and AP passing through *i*to*j* are denoted as Q_{ij} and P_{ij}. The branch's conductance is denoted as G_{ij} and the branch's susceptance is denoted as B_{ij}.

Constraints in Voltage Magnitude

For every node, there is a constraint on the magnitude of voltage, and it is depicted in Equation (24).

$$V_{-j} \le \mathrm{V}_{\overline{J,t}} \le \overline{\mathrm{V}}_{\overline{J,}} \forall \mathrm{j} \in \mathrm{N} \quad (24)$$

In Equation (3), the upper limit and lower limit of the magnitude of the voltage in node *j* are denoted as $\overline{\mathrm{V}}_j$ and V_{-j}, respectively.

Constraints in Photovoltaic Inverter Output

Photovoltaics produce electricity at the highest power by having the reactive output adjusted, and this is so as to ensure financial viability. The constraints in Equation (25) below have to be considered by the AP.

$$P_t^{pv} = P_{MPPT,t}^{pv} \quad (25)$$

Here, the AP output of the photovoltaic system, which operates and tracks points in the highest power, is represented as $P_{MPPT,}^{TPV.}$The photovoltaic inverter's RP output must follow the constraints in power factor and capacity given in Equations (26) and (27),

$$|Q_t^{pv}| \leq \sqrt{(S^{pv})^2 - \left(P_{MPPT,t}^{pv}\right)^2} \quad (26)$$

$$0.95 \leq \cos\left((\theta_i^{PP}\right) \leq 1 \quad (27)$$

Here, the photovoltaic inverter's respective power is denoted asS^{pv}. At the connection point of the photovoltaic grid, the power factor is denoted as θ_i^{PP}.

Constraints in Energy Storage Inverter Output

Equations (28) and (29) provide the constraints on the output of energy storage inverters,

$$|Q_t^{DESS}| \leq \sqrt{(S^{DESS})^2 - (P_t^{DESS})^2} \quad (28)$$

$$0.95 \leq \cos\left(\theta_t^{DESS}\right) \leq 1 \quad (29)$$

OLTC, CB, and VR's Limitations on the Number of Operations

The various limitation is given in Equations (30) to (36)

$$\begin{cases} N_t^{OLTC} \leq \bar{N}^{OLTC} \\ N_t^{CB} \leq \bar{N}^{CB} \\ N_t^{VR} \leq \bar{N}^{VR} \end{cases} \quad (30)$$

$$N_t^{OLTC} = \sum_{t'=0}^{t} n_{t'}^{OLTC} \quad (31)$$

$$n_t^{OLTC} = \begin{cases} 1, if: T_t^{OLTC} - T_{t-1}^{OLTC} \neq 0 \\ 0, if: T_t^{OLTC} - T_{t-1}^{OLTC} = 0 \end{cases} \quad (32)$$

$$N_t^{CB} = \sum_{t'=0}^{t} n_{t'}^{CB} \quad (33)$$

$$n_t^{CB} = \begin{cases} 1, if: T_t^{CB} - T_{t-1}^{CB} \neq 0 \\ 0, if: T_t^{CB} - T_{t-1}^{CB} = 0 \end{cases} \quad (34)$$

$$N_t^{VR} = \sum_{t'=0}^{t} n_{t'}^{VR} \quad (35)$$

$$n_t^{VR} = \begin{cases} 1, if: T_t^{VR} - T_{t-1}^{VR} \neq 0 \\ 0, if: T_t^{VR} - T_{t-1}^{VR} = 0 \end{cases} \quad (36)$$

Here, OLTC, CB, and VR's upper limits of counts of action are denoted as $\bar{N}^{OLTC}$,$\bar{N}^{CB}$, and $\bar{N}^{VR}$, respectively.

To check and record the changes in the position of the tap of OLTC at time *t*, is denoted as n_t^{OLTC}.

At *t*, the position of the tap of OLTC is depicted as T_t^{OLTC}. If the position of CB changes at *t*, then it is recorded with the help of n_t^{CB}. The position of CB is depicted as T_t^{CB}.

If the position of the VR changes at *t*, then it is recorded by $n_t^{VR,}$and T_t^{VR}, indicates the VR's position at *t*.

3.4. Computational Complexity of SA-STO

Time Complexity: SA-STO is a metaheuristic algorithm, similar in structure to well-known algorithms like PSO, GA, and DE. It operates on a population of candidate solutions and runs them over generations. Each iteration involves evaluating p candidates across d =5 dimensions (i.e. the tuning variables μ, λ, K_P, K_D, and K_I).

3.4.1. Space Complexity

Since SA STO retains p candidate solutions, each consisting of d variables in memory, the space complexity is $O(p \times d)$, which is consistent with typical metaheuristic storage requirements.

Table 2. Theoretical computational complexity of the SA-STO algorithm

Complexity Type	Expression	Computed Value
Time (per iteration)	*O(p×d)*	20×5=100
Total time	*O(g×p×d)*	100×20×5=10,000 fitness evaluations
Space Complexity	*O(p×d)*	20×5=100 parameters stored

Table 2 summarizing the theoretical computational complexity of the SA-STO algorithm based on standard metaheuristic analysis, along with recommended parameter values.

3.4.2. Practical Considerations

Fitness evaluations (calculating voltage deviation and power loss) are the main source of time burden, and they scale linearly with dimension d. In contrast, other overheads (like candidate tracking or updating) are negligible. A classic trade-off in metaheuristic algorithms is that while increasing the population size p or number of iterations g can enhance solution quality and convergence robustness, doing so also lengthens runtime.

4. Result and Discussion

This section examines and assesses the effectiveness of the SA-STO approach, which is now being developed to attain control stability in VPPs. The MATLAB-Simulink tool has been used to implement the proposed framework. This procedure relied on MATLAB R2022a and Windows 10 Pro. The 8 GB of RAM is paired with the Intel ® Core (TM) i3-6098P CPU running at 3.60 GHz. The KP, KI, and KD parameters of the controllers were found to have upper and lower limits ranging from -1 to +1 after an extensive process of trial and error. The fractional parameters λ and μ are chosen between 0 and 2. The simulations were done using optimization methods up to 200 iterations in order to reduce J. Solar, wind, and battery production, grid performance, power loss, and Total Harmonic Distortion (THD) are among the measures examined. After that, we evaluate the performance

of the improved PI- FOPID controller compared to classic FOPID, PID, and PI controllers. The convergence behavior of an optimization method is shown in Figure 4, where the x-axis represents the number of iterations, and the y-axis reflects the greatest fitness value achieved at this point. Initially, the fitness value is rather high, approximately 12×10412 \times 10^4, but it drops down fast in the first iterations, indicating that the algorithm discovers much-improved solutions rather soon. The improvement rate decreases as iterations continue, signifying a shift from exploration to exploitation. The curve flattens out around about 100 iterations, which means the algorithm is getting close to finding an optimum or almost ideal solution. The optimal solution is fine-tuned after early quick convergence, characteristic of metaheuristic optimization approaches of Self-Adaptive Siberian Tiger Optimization (SA-STO). With the goal function effectively minimized (or maximized) and the best-found solution progressively improved over time, the graph's overall trend indicates that the optimization process is successful.

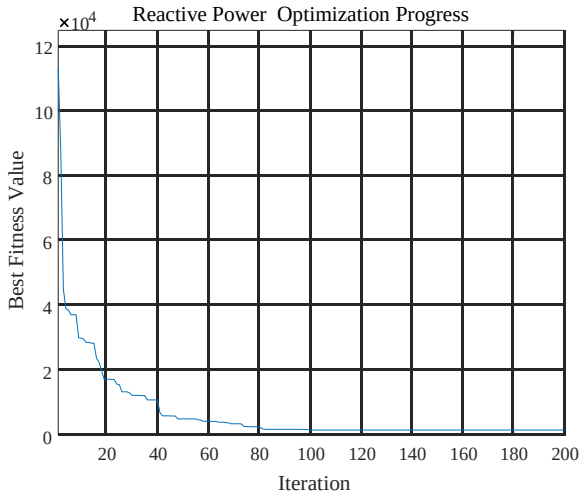

Fig. 4 SA-STO's flow diagram

Total Harmonic Distortion (THD) is compared in Figure 5 across several control models, such as PI, PID, FOPID, Phase 1, and Phase 2. According to the data, the PI controller has the best harmonic performance with a THD of 5.68%, while the PID controller comes in second with 4.62%. Further reduction of THD to 3.968% by the FOPID controller indicates improved harmonic suppression. The Phase2 model achieves the lowest Total Harmonic Distortion (THD) value of 3.63%, whereas the Phase1 model reaches a value of 3.74%, demonstrating better performance in reducing distortions.

This pattern indicates that more significant harmonic reduction enhances system stability and efficiency as the control method progresses. Regarding power electronics, motor drives, and grid systems applications that need accurate harmonic mitigation, the results show how successful sophisticated control approaches are in enhancing system performance.

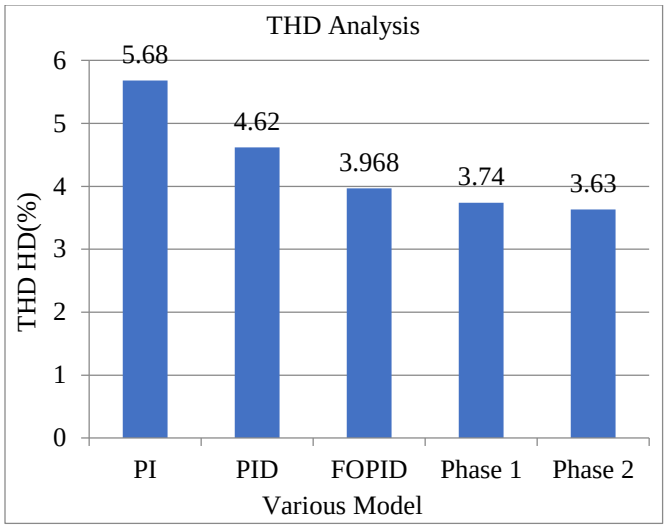

Fig. 5 Performance comparison of THD

Figure 6 shows the difference between pre- and post-optimization power loss (kW). In contrast to the Optimized Loss, which drops to 1-2 kW, the Initial Loss is around 12 kW, which is much larger. An optimization approach that successfully reduces power losses, as shown by this significant drop, might use more sophisticated control algorithms, energy-efficient methods, or better system designs. There will be less energy wasted and better system performance due to the optimization process, which probably improves power distribution efficiency. Applications like power grids, renewable energy systems, and industrial automation are vital for these advancements since reducing power loss has an immediate impact on sustainability and cost savings.

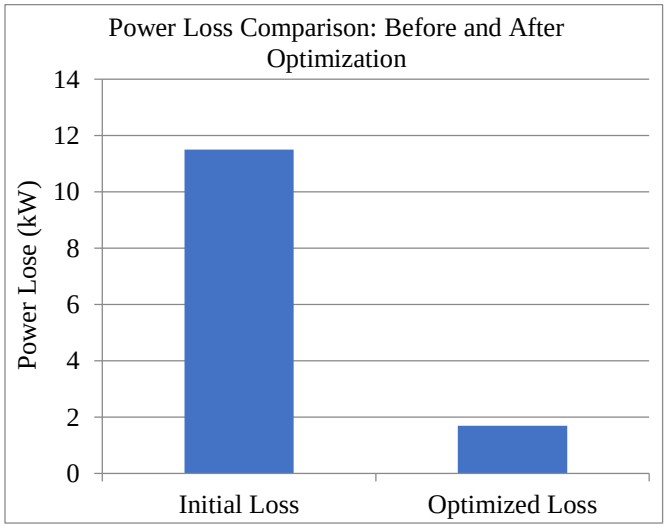

Fig. 6 Performance comparison of power loss

In Figure 7, the plotted data show the evolution of the system's reaction over time, with seconds on the x-axis and kilowatts (kW) on the y-axis. The red dashed line shows the

steady-state value, while the blue curve shows the system's response. The system output stays far below the expected steady-state value, implying an undershoot rather than a usual overshoot. The overshoot is labelled as -26.11%. Based on this reaction, the system seems to have trouble reaching a steady state or performing slowly due to undersampling. This behaviour might be caused by too cautious control settings, too much dampening, or external limits on the system's ability to function. When applied to real-world scenarios, this might mean energy distribution is inefficient, power systems have a delayed dynamic reaction, or industrial control systems are underperforming. Developing a more responsive optimization technique, reducing system latency, or adjusting the control settings to increase performance may be required.

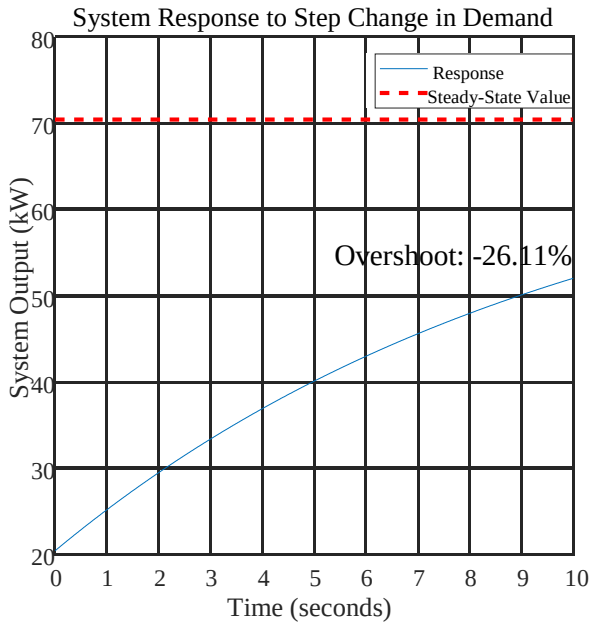

Fig. 7 System response to step change in demand

An optimization algorithm's convergence behaviour is shown in Figure 8, with the number of iterations on the x-axis and the best fitness value, expressed in terms of voltage deviation, on the y-axis. The fitness value changes as the iteration progresses, as the blue curve shows. A considerable voltage deviation is indicated by an initially relatively high fitness value. There is a noticeable decline in the fitness value within the first fifty iterations, suggesting that the optimization method successfully reduces the deviation as iterations pass. Once the algorithm reaches this stage, iterative improvements slow down, and the fitness value stabilizes after around 150 iterations, indicating that an optimum or near-optimal solution has been found.

The optimization strategy effectively decreases voltage variation, which is critical for applications like power system stability and voltage control, as shown in this Figure. The smooth convergence pattern implies efficient parameter tuning and resilient algorithmic performance, which reflects a well-behaved optimization process without notable oscillations.

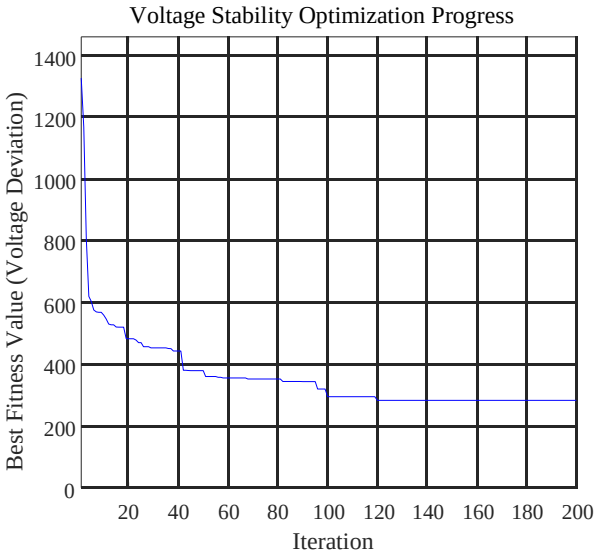

Fig. 8 Voltage stability optimization process using SA-STO

5. Conclusion

This research aimed to provide the SA-STO algorithm, which stands for Self-Adaptive Siberian Tiger Optimization, to improve VPPs' voltage management and reactive power supply. The proposed approach improves grid stability by responding to operational situations in real time with optimization parameters. The SA-STO algorithm outperformed traditional optimization techniques regarding computing efficiency, reactive power compensation, and voltage control by including self-adaptive processes. By reducing voltage variations and improving reactive power management, the SA-STO algorithm guarantees efficient and dependable energy distribution in VPPs, as shown in simulation results. It is a reliable option for modern power networks because of its flexibility in responding to changing grid circumstances. Finally, SA-STO optimizes power systems in a way that is scalable, efficient, and intelligent, which helps build energy networks that are more sustainable and stronger. Future work might investigate its integration with real-time grid monitoring systems and machine learning approaches to improve performance and flexibility in dynamic energy conditions.

References

[1] Daiva Stanelyte, and Virginijus Radziukynas, "Review of Voltage and Reactive Power Control Algorithms in Electrical Distribution Networks," *Energies*, vol. 13, no. 1, pp. 1-26, 2020. [CrossRef] [Google Scholar] [Publisher Link]

[2] Tomoya Enokido, Ailixier Aikebaier, and Makoto Takizawa, "Computation and Transmission Rate Based Algorithm for Reducing the Total Power Consumption," *2011 International Conference on Complex, Intelligent, and Software Intensive Systems*, Seoul, Korea (South), pp. 233-240, 2011. [CrossRef] [Google Scholar] [Publisher Link]

[3] Bianca Goia, Tudor Cioara, and Ionut Anghel, "Virtual Power Plant Optimization in Smart Grids: A Narrative Review," *Future Internet*, vol. 14, no. 5, pp. 1-22, 2022. [CrossRef] [Google Scholar] [Publisher Link]

[4] Taher Niknam et al., "Multiobjective Optimal Reactive Power Dispatch and Voltage Control: A New Opposition-Based Self-Adaptive Modified Gravitational Search Algorithm," *IEEE Systems Journal*, vol. 7, no. 4, pp. 742-753, 2013. [CrossRef] [Google Scholar] [Publisher Link]

[5] G. Suresh, and D. Lenine, "Gaps of Indian Electrical Energy Sector and Its Optimal Mitigation by Using Optimal Utilization of Indian Renewable Energy Policy with the Help of the P&O MPPT Technique," *Archives for Technical Sciences*, vol. 31, no. 2, pp. 94-115, 2024. [CrossRef] [Google Scholar] [Publisher Link]

[6] Giuseppe Fusco, Mario Russo, and MicheleDeSantis, "Decentralized Voltage Control in Active Distribution Systems: Features and Open Issues," *Energies*, vol. 14, no. 9, pp. 1-31, 2021. [CrossRef] [Google Scholar] [Publisher Link]

[7] Kun Wang et al., "Flexible Resource Dynamic Aggregation Regulation Method of Virtual Power Plant to Ensure More Renewable Energy Generation," *Process Safety and Environmental Protection*, vol. 180, pp. 339-350, 2023. [CrossRef] [Google Scholar] [Publisher Link]

[8] Abeer A. Kadhim, Samir J. Mohammed, and Qais Al-Gayem, "DVB-T2 Energy and Spectral Efficiency Trade-off Optimization based on Genetic Algorithm," *Journal of Internet Services and Information Security*, vol. 14, no. 3, pp. 213-225, 2024. [CrossRef] [Google Scholar] [Publisher Link]

[9] Subhojit Dawn et al., "Integration of Renewable Energy in Microgrids and Smart Grids in Deregulated Power Systems: A Comparative Exploration," *Advanced Energy and Sustainability Research*, vol. 5, no. 10, pp. 1-23, 2024. [CrossRef] [Google Scholar] [Publisher Link]

[10] Tomasz Sikorski et al., "A Case Study on Distributed Energy Resources and Energy-Storage Systems in a Virtual Power Plant Concept: Technical Aspects," *Energies*, vol. 13, no. 12, pp. 1-30, 2020. [CrossRef] [Google Scholar] [Publisher Link]

[11] Anju Rajput et al., "Design of Novel High-Speed Energy-Efficient Robust 4:2 Compressor," *Journal of VLSI Circuits and Systems*, vol. 6, no. 2, pp. 53-64, 2024. [Google Scholar] [Publisher Link]

[12] Junhui Huang, Hui Li, and Zhaoyun Zhang, "Review of Virtual Power Plant Response Capability Assessment and Optimization Dispatch," *Technologies*, vol. 13, no. 6, pp. 1-31, 2025. [CrossRef] [Google Scholar] [Publisher Link]

[13] Bogdan Marinescu et al., "Dynamic Virtual Power Plant: A New Concept for Grid Integration of Renewable Energy Sources," *IEEE Access*, vol. 10, pp. 104980-104995, 2022. [CrossRef] [Google Scholar] [Publisher Link]

[14] G.A. Bakare et al., "Comparative Application of Differential Evolution and Particle Swarm Techniques to Reactive Power and Voltage Control," *2007 International Conference on Intelligent Systems Applications to Power Systems*, Kaohsiung, Taiwan, pp. 1-6, 2007. [CrossRef] [Google Scholar] [Publisher Link]

[15] Dimitris Mourtzis, and John Angelopoulos, "Reactive Power Optimization Based on the Application of an Improved Particle Swarm Optimization Algorithm," *Machines*, vol. 11, no. 7, pp. 1-20, 2023. [CrossRef] [Google Scholar] [Publisher Link]

[16] Hossein Nezamabadi, and Mehrdad Setayesh Nazar, "Arbitrage Strategy of Virtual Power Plants in Energy, Spinning Reserve and Reactive Power Markets," *IET Generation, Transmission & Distribution*, vol. 10, no. 3, pp. 750-763, 2016. [CrossRef] [Google Scholar] [Publisher Link]

[17] Md. Shahid Iqbal et al., "A Hybrid Optimization Algorithm for Improving Load Frequency Control in Interconnected Power Systems," *Expert Systems with Applications*, vol. 249, pp. 1-16, 2024. [CrossRef] [Google Scholar] [Publisher Link]

[18] Neethu Elizabeth Michael et al., "Reactive Power Compensation Using Electric Vehicle and Data Center by Integrating Virtual Power Plan," *Electric Power Components and Systems*, vol. 50, no. 4-5, pp. 245-255, 2022. [CrossRef] [Google Scholar] [Publisher Link]

[19] Duncan S. Callaway, and Ian A. Hiskens, "Achieving Controllability of Electric Loads," *Proceedings of the IEEE*, vol. 99, no. 1, pp. 184-199, 2011. [CrossRef] [Google Scholar] [Publisher Link]

[20] Mohabbat Vafa, Mohammad Hossain Ershadi, and Behdad Arandian, "Robust Operation of Renewable Virtual Power Plant in Intelligent Distribution System Considering Active and Reactive Ancillary Services Markets," *Scientific Reports*, vol. 15, no. 1, pp. 1-24, 2025. [CrossRef] [Google Scholar] [Publisher Link]

[21] Abdallah Mohammed et al., "A Comprehensive Review of Advancements and Challenges in Reactive Power Planning for Microgrids," *Energy Informatics*, vol. 7, no. 1, pp. 1-27, 2024. [CrossRef] [Google Scholar] [Publisher Link]

[22] Mohammad Almomani, Ahmed Alkhonain, and Venkataramana Ajjarapu, "Extended Sensitivity-Aware Reactive Power Dispatch Algorithm for Smart Inverters with Multiple Control Modes," *arXiv Preprint*, pp. 1-5, 2025. [CrossRef] [Google Scholar] [Publisher Link]

[23] Moein Esfahani et al., "A Distributed VPP-Integrated Co-Optimization Framework for Energy Scheduling, Frequency Regulation, and Voltage Support Using Data-Driven Distributionally Robust Optimization with Wasserstein Metric," *Applied Energy*, vol. 361, pp. 1-20, 2024. [CrossRef] [Google Scholar] [Publisher Link]